Published in final edited form as:
Plant J. 2014 February ; 77(4): 558–567. doi:10.1111/tpj.12401.

Association of cytochrome b_5 with ETR1 ethylene receptor signaling through RTE1 in Arabidopsis

Jianhong Chang[1,†], **John M. Clay**[†], and **Caren Chang**[*]
Department of Cell Biology and Molecular Genetics, University of Maryland, College Park, MD 20742, USA

Jianhong Chang: changjh99@gmail.com; John M. Clay: jclay421@umd.edu

Summary

Ethylene plays important roles in plant growth, development and stress responses and is perceived by a family of receptors that repress ethylene responses when ethylene is absent. Repression by the ethylene receptor ETR1 depends on an integral membrane protein, REVERSION-TO-ETHYLENE SENSITIVITY1 (RTE1), which acts upstream of ETR1 in the endoplasmic reticulum (ER) membrane and Golgi apparatus. To investigate RTE1 function, we screened for RTE1-interacting proteins using the yeast split ubiquitin assay, which yielded the ER-localized cytochrome b_5 (Cb5) isoform D. Cb5s are small hemoproteins that carry out electron transfer reactions in all eukaryotes, but their roles in plants are relatively uncharacterized. Using bimolecular fluorescence complementation (BiFC), we found that all four ER-localized Arabidopsis Cb5 isoforms (AtCb5-B, -C, -D and –E) can interact with RTE1 in plant cells. In support of this interaction, *atcb5* mutants exhibited phenotypic parallels with *rte1* mutants in Arabidopsis. Phenotypes included partial suppression of *etr1-2* ethylene insensitivity and no suppression of *RTE1*-independent ethylene receptor isoforms. Single loss-of-function mutants, *atcb5-b*, *-c* and *-d*, appeared similar to the wild type, but double mutant combinations displayed a slight ethylene hypersensitivity. Overexpression of *AtCb5-D* conferred reduced ethylene sensitivity similar to that conferred by *RTE1* overexpression, and genetic analyses suggested that *AtCb5-D* acts upstream of *RTE1* in ethylene response. These findings uncover an unexpected role for Cb5, in which Cb5 and RTE1 are functional partners in promoting ETR1-mediated repression of ethylene signaling.

Keywords

ethylene; cytochrome b_5; RTE1; ethylene receptor; ETR1; yeast split ubiquitin; protein-protein interaction; signaling; redox; *Arabidopsis thaliana*

[*]Corresponding author: Caren Chang, Department of Cell Biology and Molecular Genetics, Bioscience Research Building, Bldg 413, University of Maryland, College Park, MD 20742, USA, Phone: 301-405-1643, Fax: 301-314-1248, carenc@umd.edu.
[†]These authors contributed equally to this work
[1]Current Address: Department of Molecular Biomedical Sciences, College of Veterinary Medicine, North Carolina State University, Raleigh, NC 27606, USA

Introduction

The gaseous plant hormone ethylene affects many aspects of plant growth and development including seedling growth, fruit ripening, abscission, senescence and responses to biotic and abiotic stresses (Abeles et al., 1992). Ethylene is perceived by a family of ethylene receptors that are derived from two-component histidine protein kinase receptors (Bleecker and Kende, 2000). The ethylene receptors, which reside at the endoplasmic reticulum (ER) membrane (Chen et al., 2002; Ma et al., 2006; Zhong et al., 2008) and possibly at the Golgi apparatus (Dong et al., 2008), are disulfide-linked homodimers that form higher order multimeric complexes with each other (Gao et al., 2008). In the absence of ethylene binding, the receptors repress ethylene responses through activation of the CTR1 protein kinase by an unknown mechanism, and when ethylene is bound to the receptors, CTR1 is inactivated, leading to ethylene responses (Wang et al., 2006).

ETR1, one of the five ethylene receptors in *Arabidopsis thaliana*, is dependent on an upstream-acting ER/Golgi apparatus membrane protein, RTE1, which promotes ETR1 signaling (Resnick et al., 2006; Resnick et al., 2008; Zhou et al., 2008; Dong et al., 2008; Rivarola et al., 2009). It was proposed that RTE1 serves as a molecular chaperone that stabilizes or promotes the active signaling conformation of ETR1, which represses ethylene responses (Resnick et al., 2008). *rte1* loss-of-function mutants, such as the severe loss-of-function mutant *rte1-2* and the *rte1-3* null mutant, have an ethylene hypersensitive phenotype similar to that displayed by an *etr1* loss-of-function mutant and can suppress a number of dominant *etr1* alleles that confer ethylene insensitivity (Resnick et al., 2006; Resnick et al., 2008). Consistent with *RTE1* being an upstream regulator of *ETR1*, overexpression of *RTE1* confers reduced ethylene sensitivity, but only in the presence of *ETR1* (Zhou et al., 2007). The tomato *RTE1* homologs, *GREEN-RIPE* and *GREEN-RIPE LIKE1*, similarly confer reduced ethylene sensitivity when overexpressed (Barry and Giovannoni, 2006; Ma et al., 2012).

The molecular mechanism of *RTE1* action is unknown and despite the conservation of RTE1 in plants and metazoans (Resnick et al., 2006), the only identified target of RTE1 is the Arabidopsis ETR1 ethylene receptor. Here, we find that RTE1 physically associates with cytochrome *b5*. Genetic analyses indicate that cytochrome *b5* plays a functional role similar to that of RTE1 in promoting ETR1 signaling in Arabidopsis.

Results

Interaction between cytochrome *b5* isoforms and RTE1

To identify potential RTE1-interacting proteins, we screened an Arabidopsis inflorescence cDNA library with a full-length RTE1 bait protein using the yeast split ubiquitin system (Stagljar et al., 1998), an assay based on reconstitution of ubiquitin (Ub) protein halves (Cub and Nub) in the cytosol. Prior to screening, we determined that the RTE1 bait fusion was localized primarily to the yeast ER membrane with the C-terminus localized in the yeast cytoplasm as required by the assay (Figure S1). We screened 3.2×10^5 colonies, and out of several initial positives that we isolated and retested, one clone that remained positive encoded the C-terminus of cytochrome b_5 (Cb5) isoform D (AtCb5-D). Cb5s comprise a

family of ubiquitous conserved hemoproteins that carry out electron transfer (Schenkman and Jansson, 2003). Arabidopsis has five Cb5 isoforms (AtCb5-A, At1g26340; -B, At2g32720; -C, At2g46650; -D, At5g48810; -E, At5g53560) with amino acid identity ranging from 40-70% (Nagano et al., 2009). All five possess the conserved features of Cb5s: an N-terminal predicted cytosolic heme-binding domain and a C-terminal predicted transmembrane domain that anchors the protein to either the ER or mitochondria/ chloroplast, followed by a short luminal tail (Maggio et al., 2007; Kutay et al., 1993). The AtCb5-D isoform, which consists of 140 residues, localizes to the endoplasmic reticulum (ER) membrane (Maggio et al., 2007). The *AtCb5-D* clone that was isolated from the screen encodes the last 38 residues consisting of the transmembrane domain preceded by 11 cytosolic residues and followed by an 11-residue luminal tail (Figure 1a). We subsequently cloned the full-length *AtCb5-D* cDNA and showed that it displays a similar interaction with RTE1 (Figure 1a,b). AtCb5-D also interacted with Arabidopsis RTE1-HOMOLOG (RTH) (Figure S2), which shares 51% amino acid identity with RTE1, but does not appear to have the same effect on ethylene signaling as RTE1 (Rivarola et al., 2009).

Using the yeast split ubiquitin assay, we found that the four other AtCb5 isoforms interacted with RTE1 as well. Isoforms B, C and E, which are thought to be ER-localized (Nagano et al., 2009; Hwang et al., 2004), gave the strongest interaction, whereas isoform A, which localizes to the chloroplast envelope (Maggio et al., 2007), gave the weakest. There was no interaction with an ER-membrane localized cation transporter, CHX20 (Padmanaban et al., 2007), which was used as a negative control (Figure 1b).

We next examined these interactions *in planta* using bimolecular fluorescence complementation (BiFC). The coding sequences of the YFP halves, cYFP and/or nYFP, were fused to the full-length coding sequences of *RTE1* and the *AtCb5*s at the corresponding N-terminus of each protein. Cb5 and RTE1 both have cytosolic N-termini (Maggio et al., 2007; Dong et al., 2010), and we previously showed the RTE1 tagged with RFP at its N-terminus is capable of rescuing an *rte1* loss-of-function mutant (Dong et al., 2008). When we transiently expressed cYFP-RTE1 in tobacco leaf epidermal cells, paired with either nYFP-AtCb5-B, -C, -D or -E, fluorescence was readily detected (Figure 1c). As expected, we did not detect interaction between cYFP-RTE1 and nYFP-AtCb5-A, because RTE1 localizes to the ER/Golgi apparatus in plant cells (Dong et al., 2008), whereas AtCb5-A localizes to the chloroplast envelope (Maggio et al., 2007). The observed interaction between RTE1 and AtCb5-A in the yeast split ubiquitin assay might have been due to localization of AtCb5-A to the ER in yeast cells, similar to the ER mislocalization of an *Aleurites fordii* (tung tree) mitochondrial Cb5 isoform when expressed in yeast (Hwang et al. 2004).

Since RTE1 can interact with ETR1, we also tested for interaction between cYFP-AtCb5-D and ETR1-nYFP (using the interaction of cYFP-AtCb5-D and nYFP-RTE1 as a positive control), but did not detect interaction. We similarly tested for, but did not detect, interaction of AtCb5-D with CTR1, which is a protein kinase in the ETR1 receptor complex (Gao et al., 2003).

Ethylene response in *atcb5-b, -c* and *-d* mutants

Using existing T-DNA insertion mutants of *AtCb5-B, -C* and *–D*, we investigated whether *AtCb5*s play a role similar to that of *RTE1* in repressing ethylene responses. (Mutants of *AtCb5-E* were not available at the time of this study.) RT-PCR analysis indicated that *atcb5-b* is a partial loss-of-function mutant, while *atcb5-c* and *atcb5-d* are stronger loss-of-function mutants (Figure S3). The three mutants showed no obvious defects in the seedling triple response compared to the wild type (Figure 2a,b). We also constructed and analyzed two double mutants, *atcb5-b/c* and *atcb5-b/d*. In the triple response assay, the hypocotyls of the double mutants were slightly shorter than that of the wild type when germinated on a low dose (0.5μM) of the ethylene precursor 1-aminocyclopropane-1-carboxylic acid (ACC), although not as short as that of *rte1-3* (Figure 2a,b). There was also a slight hypocotyl shortening in the absence of ACC treatment, as seen for *rte1-3* (Figure 2b). Alleviation of this shortening by treatment with the ethylene biosynthesis inhibitor aminoethoxyvinylglycine (AVG) (Figure 2c) suggested that the shortening was caused in part by hypersensitivity to endogenously produced ethylene. Although the phenotypes were weak, these results suggest that *AtCb5-B, -C* and *-D* have overlapping or redundant roles in repressing ethylene response.

We next tested whether overexpression of *AtCb5-D* by the CaMV 35S promoter would confer the opposite phenotype – reduced sensitivity to ethylene – in wild-type Arabidopsis. Overexpression was confirmed by RT-PCR for two independent lines (Figure 2d), and both lines showed reduced ethylene sensitivity, which was similar to that conferred by overexpression of *RTE1* (Figure 2e,f). This suggests that *AtCb5-D* has a similar effect on ethylene response as *RTE1*.

RTE1-dependent *etr1* alleles that confer ethylene insensitivity are similarly dependent on *AtCb5*

Since *rte1* mutations were originally identified by the ability to suppress the ethylene-insensitive phenotype of *etr1-2*, we tested whether the *atcb5-b, -c* and *-d* mutants could similarly suppress *etr1-2*. Each *etr1-2 atcb5* double mutant exhibited reduced ethylene insensitivity compared to *etr1-2* alone, as revealed by an ethylene dose response analysis (Figure 3a,b). In each case, the hypocotyl length reduction was not as great as that in the *etr1-2 rte1-3* double mutant, possibly due to functional redundancy of the *AtCb5* genes. To verify that the *etr1-2* suppressed phenotype was due to the *atcb5* mutation, we showed that the ethylene-insensitive phenotype of *etr1-2* could be fully restored by transforming the *etr1-2 atcb5-d* double mutant with either a genomic wild-type *AtCb5-D* gene fragment (including 1.9 kb of the promoter region) or the *35S-AtCb5-D* overexpression construct (Figure 3c).

We also observed partial suppression of *etr1-2* ethylene insensitivity by *atcb5-b, -c* and *-d* in adult plants, based on reduced chlorophyll content in rosette leaves (Table 1). These results indicate that the ethylene insensitivity conferred by *etr1-2* is partially dependent on *AtCb5-B, -C*, and *-D* in both seedling and adult stages, similar to *etr1-2* dependence on *RTE1* as shown in Resnick et al. (2006).

Since Resnick *et al*. (2008) found that the loss of *rte1* function reduces ethylene insensitivity in a specific set of *etr1* dominant mutant alleles, we were interested to see whether the *atcb5-d* loss-of-function mutation could suppress the same *etr1* alleles as *rte1*. To test this, we genetically crossed the *atcb5-d* mutant with five existing transgenic lines (Resnick *et al.*, 2008), each expressing a different *etr1* dominant allele that had been created by *in vitro* site-directed mutagenesis (Wang et al., 2006). Four of the substitutions (E38A, F58A, F61A, L64A) are dependent on *RTE1* for ethylene insensitivity, while one (T101A) is *RTE1*-independent (Resnick et al., 2008). Seedlings homozygous for both the *etr1* mutant transgene and *atcb5-d* were compared with seedlings of the parental *etr1* mutant transgenic lines in the presence and absence of 20 μM ACC. On ACC, the *atcb5-d* mutation was able to weakly suppress the four *RTE1*-dependent alleles, but was unable to suppress the *RTE1*-independent allele (Table 2; Figure S4). Thus, *atcb5-d* affects the same *etr1* dominant ethylene-insensitive alleles as *rte1*, consistent with *AtCb5s* playing a role similar to that of *RTE1* in promoting ETR1 ethylene receptor function.

We next tested whether the *atcb5-d* loss-of-function mutant is able to suppress dominant ethylene-insensitive mutations in other ethylene receptor genes by constructing double mutants between *atcb5-d* and two dominant ethylene-insensitive mutants, *ers1-10* and *etr2-1*, neither of which are suppressed by the *rte1-2* loss-of-function mutation (Resnick et al., 2006). As with *etr2-1 rte1-2*, the *etr2-1 atcb5-d* double mutant was identical to the *etr2-1* single mutant under a wide range of ethylene doses (Figure S5a), indicating that *atcb5-d* is unable to reduce *etr2-1* ethylene insensitivity. Likewise, *atcb5-d* failed to suppress *ers1-10* under a wide range of ethylene doses (Figure S5b), even though *ers1-10* (Alonso et al., 2003) is a weak allele. This suggests that *atcb5-d* could be specific to *ETR1*, similar to *rte1*.

AtCb5-D appears to act upstream of *RTE1* in the same pathway

To examine the genetic relationship between *AtCb5-D* and *RTE1*, we constructed the double mutant *rte1-3 atcb5-d* and the triple mutant *etr1-2 rte1-3 atcb5-d*. The *rte1-3 atcb5-d* double mutant was indistinguishable from the *rte1-3* single mutant (Figure 4a), and similarly, the *etr1-2 rte1-3 atcb5-d* triple mutant displayed the same phenotype as *etr1-2 rte1-3* (Figure S6). Thus, *AtCb5-D* and *RTE1* have no obvious synergistic or additive effects. Instead, the results are consistent with *AtCb5-D* and *RTE1* acting in the same ethylene-response pathway.

We next tested whether the *AtCb5-D* overexpression phenotype is dependent on *RTE1* or vice versa. Overexpression of either *AtCb5-D* or *RTE1* conferred reduced sensitivity to ethylene in the wild-type background. When *35S-RTE1* was transformed into the *atcb5-d* loss-of-function mutant, reduced ethylene sensitivity was not alleviated (Figure 4b,c). In contrast, when the *35S:AtCb5-D* transgene was genetically crossed from the wild-type background, in which we observed reduced ethylene sensitivity, into the *rte1-3* loss-of-function mutant, we no longer detected reduced ethylene sensitivity (Figure 4d,e). These results suggest that *AtCb5-D* is likely to act upstream of *RTE1*.

Discussion

By investigating the function of RTE1 and how RTE1 might regulate the ethylene receptor ETR1 in Arabidopsis, we found that Cb5s physically associate with RTE1 and play a role similar to that of RTE1. Genetic data suggests that Cb5s act upstream of RTE1 to negatively regulate ethylene responses through the ETR1 ethylene receptor.

Cb5s carry out electron transfer in plants, animals, fungi and purple bacteria (Schenkman and Jansson, 2003). Arabidopsis has five Cb5 isoforms (Nagano et al., 2009; Maggio et al., 2007), but functional information for these proteins in plants is relatively limited. Using BiFC in plant cells, we found that RTE1, which localizes to the ER and Golgi apparatus membranes (Dong et al., 2008), physically interacts with AtCb5-B, -C, -D and –E, but not with AtCb5-A. Interaction with AtCb5-A was not expected to occur since AtCB5-A localizes to the chloroplast envelope (Maggio et al., 2007). In contrast, AtCb5-D has been localized to the ER membrane (Maggio et al., 2007), and AtCb5-B, -C and –E are likely to localize to the ER membrane as well, since each of their tail sequences carries a conserved ER-targeting motif (-R/H-x-Y/F-) (Hwang et al., 2004), which is lacking in AtCb5-A.

Our genetic analyses revealed that AtCb5s have functional parallels with RTE1 in ethylene signaling. Most notably, the *atcb5-d* loss-of-function mutation partially suppressed *etr1-2* but did not suppress mutations in the *ETR2* or *ERS1* ethylene receptor genes. Furthermore, suppression by *atcb5-d* showed the same specificity for certain *etr1* mutant alleles as *rte1*. Unlike *rte1* loss-of-function, single *atcb5* loss-of-function mutants exhibited no obvious phenotypes; the double loss-of-function mutants, however, showed a slight degree of ethylene hypersensitivity, suggesting possible functional redundancy. Overexpression of the *AtCb5-D* gene, however, conferred reduced ethylene sensitivity to the same extent as that of *RTE1* overexpression. Based on the above findings, plus the absence of any obvious additive or synergistic effects in the *rte1 atcb5-d* double mutant, we propose that *AtCb5* and *RTE1* act in the same pathway to influence ethylene signaling. It is likely that *AtCb5*s act upstream of *RTE1*, since reduced ethylene sensitivity conferred by overexpression of *AtCb5-D* was blocked by the *rte1-3* loss-of-function mutation, whereas reduced ethylene sensitivity conferred by *RTE1* overexpression was not blocked by the *atcb5-d* loss-of-function mutation. RTE1 is capable of physically interacting with the ETR1 ethylene receptor (Dong et al., 2010), but we did not detect interaction between ETR1 and AtCb5-D. The *AtCb5* genes are normally expressed in almost all organs throughout all stages of development (Zimmermann et al., 2005), and thus their expression patterns overlap with that previously described for *RTE1* and *ETR1* (Dong et al., 2008; Hua et al., 1998; Raz and Ecker, 1999). Taken together, our results indicate that AtCb5 isoforms play a role in negatively regulating ethylene signaling, and suggest that AtCb5s act through RTE1 to repress ethylene responses specifically through the ETR1 ethylene receptor.

Exactly how AtCb5s and RTE1 could be functioning together is unclear. Cb5 serves as an electron transfer protein in a variety of oxidation/reduction reactions (Schenkman and Jansson, 2003). For example, Cb5 plays a role in lipid biosynthesis and metabolism by activating a variety of oxidases, such as desaturases and hydroxylases, through electron transfer (Vergeres and Waskell, 1995; Schenkman and Jansson, 2003; Hwang et al., 2004;

Kumar et al., 2012). AtCb5-B has been shown to physically interact with two Arabidopsis fatty acid hydroxylases, AtFAH1 and AtFAH2, which are believed to receive electrons from AtCb5s (Nagano et al., 2009; Nagano et al., 2012). In addition, the ER-localized AtCb5s interact with Bax inhibitor-1 (AtBI-1), an ER-membrane protein that prevents cell death induced by abiotic and biotic stresses (Nagona et al., 2009). The interaction of AtBI-1 with AtFAHs via AtCb5 links AtBI-1 function with fatty acid 2-hydroxylation (Nagano et al., 2009; Nagano et al., 2012). Conceivably, AtBI-1 function could also be linked to ethylene signaling through the AtCb5s interacting with RTE1 and affecting ETR1 ethylene receptor signaling. AtCb5s could interact simultaneously with RTE1 and AtBI-1; the N-terminal portion of AtCb5 interacts with AtBI-1 (Nagano et al., 2009), whereas the C-terminal portion of AtCb5 interacts with RTE1, based on our library screen.

Given the role of cytochrome b_5 as an electron transfer protein in various oxidation/reduction reactions, AtCb5 might activate RTE1 through redox modification and thus serve to link cellular redox status with ethylene signaling specifically through the ETR1 ethylene receptor isoform. This would be consistent with the finding that H_2O_2-induced stomatal closure is dependent on ETR1, and that the –SH group of Cys65 in ETR1 is required for this response (Desikan et al., 2005; Desikan et al., 2006). If RTE1 in turn carries out electron transfer, then RTE1 could possibly carry out oxidative folding of ETR1, and thus regulate signaling output by affecting ETR1 conformation as proposed by Resnick et al. (2009). Alternatively, ETR1 conformation could be highly sensitive to changes in membrane composition and fluidity that are affected by levels of unsaturation of fatty acids in membrane lipids controlled by AtCb5s.

While our findings reveal that AtCb5s play a role in ethylene signaling together with RTE1, the interaction of Cb5 with RTH (the Arabidopsis RTE1 homolog) could act on different target proteins. Similarly, in metazoans, which are not known to possess ethylene receptors, a conserved interaction between cytochrome b5s and RTE1 proteins (containing the domain of unknown function, DUF778) may have important functions unrelated to ethylene signaling. In metazoans, interestingly, Cb5 and RTE1 homologs are both down-regulated in models for neural degenerative diseases (Scherzer et al., 2003; Diao et al. 2013), suggesting that Cb5 and RTE1 may function together in these organisms as an important component in neural signaling.

Experimental Procedures

Plant Materials and Growth Conditions

The *Arabidopsis thaliana* Columbia ecotype (Col-0) was used as the wild type in all experiments. T-DNA insertion lines for *AtCb5-B* (Salk_100161) and *AtCb5-C* (Salk_027748) were obtained from the Arabidopsis Biological Resource Center (ABRC, The Ohio State University), and the T-DNA line for *AtCb5-D* (GABI_328H06) was obtained from the European Arabidopsis Stock Centre (NASC). *Nicotiana benthamiana* was used for BiFC. Plants were grown in soil under 16-hour light/8-hour dark in controlled environment chambers at 22°C under white fluorescent light. The triple response assay using ethylene gas, ACC or AVG was carried out as described previously (Resnick et al. 2006). Statistical analyses on hypocotyl lengths were performed either by the Student's t-test or by

one-way ANOVA with a 95% confidence interval in conjunction with Tukey's test, using GraphPad's Prism software to analyze samples and determine significant differences.

Yeast Split Ubiquitin Assay: Constructs and Library Screen

All plasmid clones below were constructed using the Gateway cloning system (Invitrogen) using PCR primers shown in Table S1a and then verified by DNA sequencing.

For library screening, we used the yeast split ubiquitin system that employs the cytosolic URA3 reporter (Wittke et al., 1999). The bait plasmid was constructed by PCR-amplification of the full-length *RTE1* coding sequence from an existing cDNA clone (Resnick et al., 2006), cloning the product into pDONR221 (Invitrogen) and then transferring the fragment into bait vector pMKZ, a gift from Imre Sommsich (Max-Planck-Institut für Züchtungsforschung, Köln, Germany). For library screening, we used a compatible Arabidopsis inflorescence cDNA library and yeast strain JD53, both kindly provided by I. Sommsich. To verify positives clones, the prey plasmids were isolated from candidate positive colonies and then retested in yeast.

For subsequent yeast split ubiquitin assays, we used the PLV transcriptional reporter system (Ludewig et al., 2003; Obrdlik et al., 2004), kindly provided by Wolf Frommer (Carnegie Institution of Washington, Stanford, California). The *RTE1* coding sequence in pDONR221 was transferred into bait vector pMetYCgate (Obrdlik et al. 2004). The coding sequences of the five *AtCb5* genes were PCR-amplified from cDNA clones (isoform A: GC00075; B: U17257; C: G83412; D: U09651; E; G10548) obtained from ABRC. The amplified fragments were cloned into pDONR221, verified by DNA sequencing and then transferred into the prey vector pNXgate33-3HA (Cappellaro and Boles, University of Frankfurt). Interactions were tested in yeast strain THY.AP4 on agar medium lacking leucine, tryptophan, adenine and histidine. The full-length CHX20 bait plasmid was kindly provided by Heven Sze (University of Maryland, College Park).

Yeast cells were maintained on enriched yeast extract-peptone-dextrose (YPD) agar plates or YPD liquid medium at 30°C. Solid and liquid synthetic complete (SC) media comprised 0.17% yeast nitrogen base (YNB, USBiological), 2% dextrose, 0.5% $(NH4)_2SO_4$ and amino acids. The SC medium was supplemented with 1 mg/ml 5-fluoroorotic acid (5-FOA) (USBiological) for the URA3-based system.

Bimolecular Fluorescence Complementation (BiFC): Constructs, Infiltration and Microscopy

All plasmid clones below were constructed using the Gateway cloning system (Invitrogen), except where noted, and all plasmid constructs were verified by DNA sequencing. All PCR primer sequences are shown in Table S1a. cYFP-RTE1 and ETR1-nYFP were described previously by Dong et al. (2010).

The cYFP-RTE1 clone was tested for interaction with each nYFP-AtCb5 clone (encoding the N-terminal portion of YFP fused to the N-terminus of each AtCb5 isoform), which were all generated in the same way as follows. We first fused *nYFP* (coding for residues 1-155) to the 5′ end of the *AtCb5* coding sequence by replacing a fragment of *ETR1* with the *AtCb5*

coding sequence in the existing nYFP-ETR1 plasmid (Dong et al., (2010). To accomplish this, we PCR-amplified the coding sequences using forward and reverse primers carrying the restriction sites *Asc*I and *Xho*I, and ligating (with T4 DNA ligase) the resulting product into the *Asc*I- and *Xho*I-digested nYFP-ETR1 plasmid. Using the resulting plasmid as a template, the fused sequences of nYFP-AtCb5 were then PCR-amplified and cloned into pDONR221, verified by DNA sequencing and finally transferred into binary plant transformation vector pEarleygate100 (Earley et al., 2006) containing the CaMV 35S promoter. nYFP-RTE1 was constructed in the exact same way, but using a primer carrying the restriction site *Spe*I in place of *Xho*I.

To construct the plasmid expressing cYFP-AtCb5-D, the full-length *AtCb5-D* coding sequence with a 5′ linker sequence and the C-terminal portion of the YFP molecule (amino acids 156-239) with a complementary 3′ linker sequence were PCR-amplified respectively from an *AtCb5-D* cDNA clone and the pSPYCE vector (Walter et al., 2004). Purified PCR products were then combined in a fusion PCR using a forward primer with an attB1 site complementary to the 5′ end of the cYFP coding sequence and a reverse primer with an attB2 site complementary to the 3′ end of the AtCb5-D coding sequence. The amplified product was cloned into pDONR221, verified by DNA sequencing and then transferred into the binary plant transformation vector pH2GW7 (Karimi et al., 2002) containing the CaMV 35S promoter.

The above nYFP and cYFP constructs were co-transformed into *Agrobacterium tumefaciens* strain C58C1, and selected by kanamycin and spectinomycin, respectively. For tobacco infiltration, liquid cultures of the *Agrobacteria* were prepared according to Voinnet et al. (2003) and each culture was combined with a separate liquid culture of *Agrobacterium* carrying the p19 plasmid (coding for the RNAi silencing inhibitor from the Cymbidium ringspot virus) in a 1:1 ratio, and the resulting mixtures were used to infiltrate leaves of 3-week old tobacco plants as described in Voinnet et al. (2003). Tobacco leaf pieces were directly mounted on glass slides in a drop of water, and YFP was observed using laser scanning confocal microscopy (Zeiss LSM710). For ETR1-nYFP + cYFP-AtCb5-D, we examined 30 plants, 1-2 leaves per plant. For CTR1-nYFP + cYFP-AtCb5-D, we examined 9 plants, 1-2 leaves per plant.

atcb5 Double and Triple Mutant Constructs

To create double and triple mutants, the F1 produced by the indicated crosses were allowed to self-pollinate, and the resulting F2 progeny were genotyped to identify the desired homozygous mutants. For genotyping, Arabidopsis genomic DNA was extracted using either the Phire Plant Direct PCR kit (Finnzymes) or the CTAB method (Dellaporta et al., 1983). PCR-based genotyping primers are shown in Table S1b. The *rte1-2*, *etr1-2*, *etr2-1* and *ers1-10* alleles were genotyped using CAPS or dCAPS primers as described in Resnick et al. (2006).

The double mutants *atcb5-b/c* and *atcb5-b/d* were created by crossing the corresponding single mutants with each other. To create double mutants between *atcb5-d* and ethylene receptor mutants, *atcb5-d* was crossed separately with *etr1-2*, *ers1-10* and *etr2-1*. To

construct the *etr1-2 rte1-3 atcb5-d* triple mutant, we crossed *etr1-2 atcb5-d* with the *etr1-2 rte1-3* mutant from Resnick et al. (2006).

To create the transgenic lines carrying the *etr1* mutant transgenes, the existing *etr1* mutant transgenic lines (in the wild-type Col-0 background) described in Resnick et al. (2008) were crossed with the *atcb5-d* mutant. To identify lines that were homozygous for the transgene, the F3 from self-pollinated F2 individuals were selected on Murashige and Skoog (MS) agar medium containing 50mg/l kanamycin.

RNA Extraction and Semi-quantitative RT-PCR

RNA was extracted from pooled seedlings or from rosette leaves using the RNeasy RNA extraction kit (Qiagen). cDNA was synthesized with oligo(dT) primers using the iScript cDNA synthesis kit (BioRad) and amplified using the primers shown in Table S1c.

Measuring Chlorophyll Content

Six-week old, soil-grown plants in individual pots were placed in a gas-tight and light-tight chamber. Ethylene gas was injected into the chamber (100 ppm) and incubated at 22°C. Three days later, the rosette leaves were quickly harvested, weighed and frozen in liquid nitrogen. Chlorophyll content was measured as described in Ni et al. (2009) using frozen leaves from the entire rosette. Chlorophyll a and b concentrations (mg/g) were calculated by the following formula: [(8.02×A663 + 20.20×A645)×V]/W, where V= volume of the extract (liter) and W= weight of fresh leaves (gram).

Constructs for Overexpression and Rescue of the *etr1-2 atcb5-d* Mutant

For overexpression, the coding sequence of *AtCb5-D* was transferred from pDONR221 into pN3F6H, a Gateway binary vector carrying a double CaMV 35S promoter and encoding N-terminal 3×Flag and 6×His tags from pN-TAPa (Rubio et al., 2005).

The *AtCb5-D* genomic DNA sequence was PCR-amplified from Arabidopsis genomic DNA using primers shown in Table S1d. The resulting fragment was cloned into pDONR221, verified by sequencing and transferred into the promoterless binary vector, pBGW (Karimi et al., 2002).

Agrobacterium strain GV3101 was used for plant transformation by the floral dip method (Clough and Bent, 1998). Transformants were selected with either the herbicide Finale (active ingredient glufosinate) (Bayer) or gentamycin (Sigma).

Supplementary Material

Refer to Web version on PubMed Central for supplementary material.

Acknowledgments

We thank Imre Sommsich for the cDNA library, vectors and yeast strain for the split ubiquitin library screen, Wolf Frommer for split ubiquitin vectors and yeast strains, PBL (UK) for *Agrobacterium* strain C58C1(pCH32) and P19, Nils Johnsson and Hemayet Ullah for advice on the split ubiquitin assay, Heven Sze for the CHX20 construct, Flanders Interuniversity Institute for Biotechnology (VIB) for pBGW and Amy Beavan (UMD Imaging Core) for confocal microscopy instruction. We are grateful to Jeff Liesch and Christine Hildreth for assistance with the yeast

split ubiquitin assay, Susan Joanna Martinez and Lillian Chang for valuable assistance with genotyping, Ruiqiang Chen for constructing pN3F6H, David Lin for assistance with plasmid constructs and Julie Caruana and Bram Van de Poel for assistance with statistical analyses. We thank Jennifer Shemansky and B. Van de Poel for critical reading of the manuscript. This work was supported by grants from the National Science Foundation (MCB0923796) and the National Institutes of Health (1R01GM071855) to C.C.. C.C. is supported in part by the Maryland Agricultural Experiment Station. A University of Maryland Graduate School Summer Fellowship and a University of Maryland Dean's Summer Fellowship provided partial support for J.C. and J.M.C., respectively.

References

Abeles, FB.; Morgan, PW.; Saltveit, ME, Jr. Ethylene in plant biology. 2nd. New York: Academic Press; 1992.

Alonso JM, Stepanova AN, Solano R, Wisman E, Ferrari S, Ausubel FM, Ecker JR. Five components of the ethylene-response pathway identified in a screen for weak ethylene-insensitive mutants in Arabidopsis. Proc Natl Acad Sci USA. 2003; 100:2992–2997. [PubMed: 12606727]

Barry CS, Giovannoni JJ. Ripening in the tomato Green-ripe mutant is inhibited by ectopic expression of a protein that disrupts ethylene signaling. Proc Natl Acad Sci USA. 2006; 103:7923–7928. [PubMed: 16682641]

Bleecker AB, Kende H. Ethylene: A Gaseous Signal Molecule in Plants. Annu Rev Cell Dev Biol. 2000; 16:1–18. [PubMed: 11031228]

Chen YF, Randlett MD, Findell JL, Schaller GE. Localization of the ethylene receptor ETR1 to the endoplasmic reticulum of Arabidopsis. J Biol Chem. 2002; 277:19861–19866. [PubMed: 11916973]

Clough SJ, Bent AF. Floral dip: a simplified method for Agrobacterium-mediated transformation of *Arabidopsis thaliana*. Plant J. 1998; 16:735–743. [PubMed: 10069079]

Dellaporta SL, Wood J, Hicks JB. A plant DNA minipreparation: version II. Plant Mol Biol Rep. 1983; 1:19–21.

Desikan R, Hancock JT, Bright J, Harrison J, Weir I, Hooley R, Neill S. A role for ETR1 in hydrogen peroxide signaling in stomatal guard cells. Plant Physiol. 2005; 137:831–834. [PubMed: 15761208]

Desikan R, Last K, Harrett-Williams R, Tagliavia C, Harter K, Hooley R, Hancock JT, Neill SJ. Ethylene-induced stomatal closure in Arabidopsis occurs via AtrbohF-mediated hydrogen peroxide synthesis. Plant J. 2006; 47:907–916. [PubMed: 16961732]

Diao H, Li X, Hu S. The identification of dysfunctional crosstalk of pathways in Parkinson disease. Gene. 2013; 515:159–162. [PubMed: 23178242]

Dong CH, Jang M, Scharein B, Malach A, Rivarola M, Liesch J, Groth G, Hwang I, Chang C. Molecular Association of the Arabidopsis ETR1 Ethylene Receptor and a Regulator of Ethylene Signaling, RTE1. J Biol Chem. 2010; 285:40706–40713. [PubMed: 20952388]

Dong CH, Rivarola M, Resnick JS, Maggin BD, Chang C. Subcellular colocalization of Arabidopsis RTE1 and ETR1 supports a regulatory role for RTE1 in ETR1 ethylene signaling. Plant J. 2008; 53:275–286. [PubMed: 17999643]

Gao Z, Chen YF, Randlett MD, Zhao XC, Findell JL, Kieber JJ, Schaller GE. Localization of the Raf-like kinase CTR1 to the endoplasmic reticulum of Arabidopsis through participation in ethylene receptor signaling complexes. J Biol Chem. 2003; 278:34725–34732. [PubMed: 12821658]

Gao Z, Wen C, Binder B, Chen Y, Chang J, Chiang Y, Kerris R, Chang C, Schaller GE. Heteromeric interactions among ethylene receptors mediate signaling in Arabidopsis. J Biol Chem. 2008; 283:23801–23810. [PubMed: 18577522]

Hua J, Meyerowitz EM. Ethylene responses are negatively regulated by a receptor gene family in *Arabidopsis thaliana*. Cell. 1998; 94:261–271. [PubMed: 9695954]

Hwang YT, Pelitire SM, Henderson M, Andrews DW, Dyer JM, Mullen RT. Novel targeting signals mediate the sorting of different isoforms of the tail-anchored membrane protein Cytochrome b5 to either Endoplasmic Reticulum or Mitochondria. Plant Cell. 2004; 16:3002–3019. [PubMed: 15486098]

Karimi M, Inzé D, Depicker A. GATEWAY vectors for Agrobacterium-mediated plant transformation. Trends Plant Sci. 2002; 7:193–195. [PubMed: 11992820]

Kumar R, Tran LS, Neelankandan AK, Nguyen HT. Higher plant cytochrome *b*5 polypeptides modulate fatty acid desaturation. PLoS One. 2012; 7(2):e31370. [PubMed: 22384013]

Kutay U, Hartmann E, Rapoport T. A class of membrane proteins with a C-terminal anchor. Trends in Cell Biol. 1993; 3:72–75. [PubMed: 14731773]

Ma B, Cui ML, Sun HJ, Takada K, Mori H, Kamada H, Ezura H. Subcellular localization and membrane topology of the melon ethylene receptor CmERS1. Plant Physiol. 2006; 141:587–597. [PubMed: 16617090]

Ma Q, Du W, Brandizzi F, Giovannoni J, Barry CS. Differential control of ethylene responses by GREEN-RIPE and GREEN-RIPE LIKE1 provides evidence for distinct ethylene signaling modules in Tomato. Plant Physiol. 2012; 160:1968–1984. [PubMed: 23043080]

Maggio C, Barbante A, Ferro F, Frigerio L, Pedrazzini E. Intracellular sorting of the tail-anchored protein cytochrome b5 in plants: a comparative study using different isoforms from rabbit and Arabidopsis. J of Exp Bot. 2007; 58:1365–1379. [PubMed: 17322552]

Nagano M, Ihara-Ohori Y, Imai H, Inada N, Fujimoto M, Tsutsumi N, Uchimiya H, Kawai-Yamada M. Functional association of cell death suppressor, Arabidopsis Bax inhibitor-1, with fatty acid 2-hydroxylation through cytochrome b5. Plant J. 2009; 58:122–134. [PubMed: 19054355]

Nagano M, Uchimiya H, Kawai-Yamada M. Plant sphingolipid fatty acid 2-hydroxylases have unique characters unlike their animal and fungus counterparts. Plant Signal Behav. 2012; 7:1388–1392. [PubMed: 22918503]

Ni Z, Kim ED, Chen ZJ. Chlorophyll and starch assays. Protocol Exchange. 200910.1038/protex. 2011.204

Obrdlik P, El-Bakkoury M, Hamacher T, Cappellaro C, Vilarino C, Fleischer C, Ellerbrok H, Kamuzinzi R, Ledent V, Blaudez D, Sanders D, Revuelta J, Boles E, Andre B, Frommer W. K+ channel interactions detected by a genetic system optimized for systematic studies of membrane protein interactions. Proc Natl Acad Sci USA. 2005; 101:12242–12247. [PubMed: 15299147]

Padmanaban S, Chanroj S, Kwak J, Li X, Ward JM, Sze H. Participation of Endomembrane Cation/H+ Exchanger AtCHX20 in Osmoregulation of Guard Cells. Plant Physiol. 2007; 144:82–93. [PubMed: 17337534]

Raz V, Ecker JR. Regulation of differential growth in the apical hook of Arabidopsis. Development. 1999; 126:3661–3668. [PubMed: 10409511]

Reichel C, Johnsson N. The split-ubiquitin sensor: Measuring interactions and conformational alterations of proteins *in vivo*. Methods Enzymol. 2005; 399:757–776. [PubMed: 16338394]

Resnick JS, Rivarola M, Chang C. Involvement of RTE1 in conformational changes promoting ETR1 ethylene receptor signaling in Arabidopsis. Plant J. 2008; 56:423–431. [PubMed: 18643990]

Resnick JS, Wen CK, Shockey JA, Chang C. REVERSION-TO-ETHYLENE SENSITIVITY1, a conserved gene that regulates ethylene receptor function in Arabidopsis. Proc Natl Acad Sci USA. 2006; 103:7917–7922. [PubMed: 16682642]

Rivarola M, McClellan C, Resnick J, Chang C. ETR1-specific mutations distinguish ETR1 from other Arabidopsis ethylene receptors as revealed genetic interaction with RTE1. Plant Physiol. 2009; 150:547–551. [PubMed: 19369589]

Rubio V, Shen Y, Saijo Y, Lio Y, Gusmaroli G, Dinesh-Kumar SP, Deng XW. An alternative tandem affinity purification strategy applied to Arabidopsis protein complex isolation. Plant J. 2005; 41:767–778. [PubMed: 15703063]

Schenkman JB, Jansson I. The many roles of cytochrome b5. Pharmacol Ther. 2003; 97:139–152. [PubMed: 12559387]

Scherzer C, Jensen R, Gullans S, Feany M. Gene expression changes presage neurodegenaration in a Drosophila model of Parkinson's disease. Hum Mol Genet. 2003; 12:2457–2466. [PubMed: 12915459]

Stagljar I, Korostensky C, Johnsson N, te Heesen S. A genetic system based on split-ubiquitin for the analysis of interactions between membrane proteins in vivo. Proc Natl Acad Sci USA. 1998; 95:5187–5192. [PubMed: 9560251]

Vergeres G, Waskell L. Cytochrome b5, its functions, structure and membrane topology. Biochimie. 1995; 77:604–620. [PubMed: 8589071]

Voinnet O, Rivas S, Mestre P, Baulcombe D. An enhanced transient expression system in plants based on suppression of gene silencing by the p19 protein of tomato bushy stunt virus. Plant J. 2003; 33:949–956. [PubMed: 12609035]

Walter M, Chaban C, Schütze K, Batistic O, Weckermann K, Näke C, Dragica B, Grefen C, Schumacher K, Oecking C, Harter K, Kudla J. Visualization of protein interactions in living plant cells using bimolecular fluorescence complementation. Plant J. 2004; 40:428–438. [PubMed: 15469500]

Wang W, Esch JJ, Shiu SH, Agula H, Binder BM, Chang C, Patterson SE, Bleecker AB. Identification of important regions for ethylene binding and signaling in the transmembrane domain of the ETR1 ethylene receptor of Arabidopsis. Plant Cell. 2006; 18:3429–3442. [PubMed: 17189345]

Wittke S, Lewke N, Muller S, Johnsson N. Probing the molecular environment of membrane proteins in vivo. Mol Biol Cell. 1999; 10:2519–2530. [PubMed: 10436009]

Zhong S, Lin Z, Grierson D. Tomato ethylene receptor-CTR interactions: visualization of NEVER-RIPE interactions with multiple CTRs at the endoplasmic reticulum. J Exp Bot. 2008; 59:965–972. [PubMed: 18349053]

Zhou X, Liu Q, Xie F, Wen C. RTE1 is a Golgi-associated and ETR1-dependent negative regulator of ethylene responses. Plant Physiol. 2007; 145:75–86. [PubMed: 17644624]

Zimmermann P, Hennig L, Gruissem W. Gene-expression analysis and network discovery using Genevestigator. Trends Plant Sci. 2005; 10:407–409. [PubMed: 16081312]

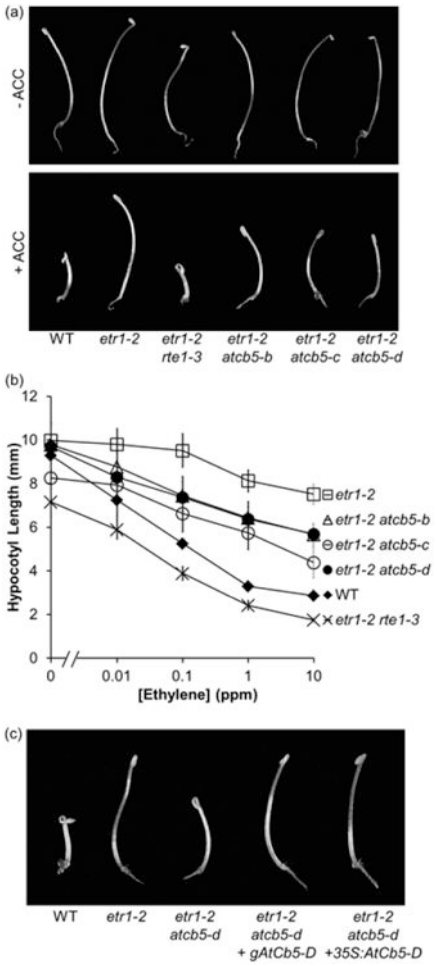

Figure 1. Arabidopsis RTE1 interacts with Arabidopsis Cb5 isoforms

(a) Schematic of RTE1 and AtCb5-D protein domains. RTE1 has at least two predicted transmembrane domains (TMs) indicated on the diagram (Resnick et al. 2006; Dong et al., 2010). AtCb5-D has a conserved heme-binding motif (solid bar) and a single TM. Using full-length RTE1 as the bait in a yeast split ubiquitin library screen, a fragment encoding the last 38 residues of AtCb5-D was isolated.

(b) Interaction between RTE1 and AtCb5 isoforms in the yeast split ubiquitin assay. Bait proteins RTE1, CHX20 (an ER-localized cation transporter used as a negative control) and the empty bait vector (negative control) were paired with each of the five AtCb5 isoforms or an empty prey vector. Yeast viability is shown on medium lacking leucine and tryptophan (-LW), while interaction is indicated by growth on medium lacking leucine, tryptophan, histidine and alanine (-LWHA). Undiluted and 1:10 diluted liquid cultures were spotted on the indicated plates and incubated for 3 days (-LW) or 5 days (-LWHA) at 30°C.

(c) Interaction of RTE1 and AtCb5 isoforms in tobacco leaf epidermal cells shown by BiFC. Constructs expressing the N- and C-terminal halves of YFP fused to the N-terminus of the AtCb5s and RTE1, respectively, were co-infiltrated into leaves of tobacco plants. YFP and chlorophyll signals were detected by laser scanning confocal microscopy at 520-550 nm and 650 nm, respectively. Scale bar = 20 μm.

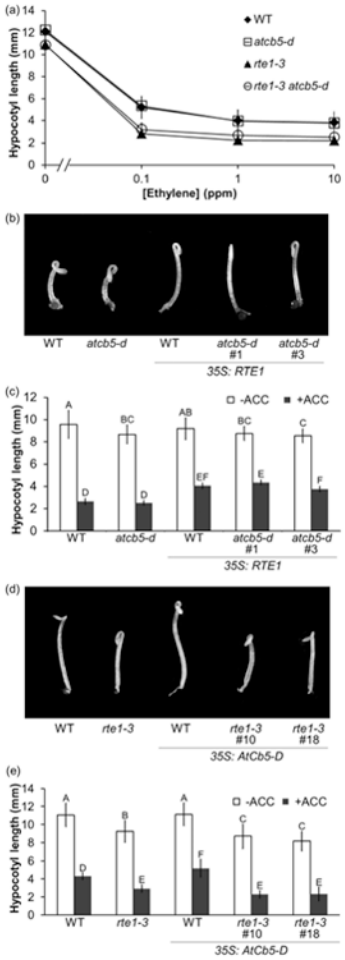

Figure 2. *atcb5* mutant alleles confer enhanced ethylene sensitivity, whereas overexpression of the wild-type *AtCb5-D* gene confers reduced ethylene sensitivity

(a) *atcb5* double mutants exhibit a slight enhanced ethylene sensitivity as compared to single *atcb5* mutants. Representative seedlings are shown for the *atcb5* single and double mutants alongside the wild type and the *rte1-3* mutant. Seedlings were germinated for 4 days in the dark on a low dose of ACC (0.5 μM).

(b) Hypocotyl lengths of 4-day old etiolated seedlings treated with or without 0.5 μM ACC suggest a slight enhanced sensitivity to ethylene in *atcb5* double mutants. The mean ± SD is shown for 16-33 seedlings per genotype for each treatment. Significant differences ($p<0.05$) between measurements are indicated by different letters above the bars.

(c) Alleviation of hypocotyl shortening by the ethylene biosynthesis inhibitor AVG in 4-day old etiolated seedlings of *atcb5* double mutants. Seedlings were germinated in the presence or absence of the ethylene biosynthesis inhibitor 10 μM AVG (without ACC). The mean ± SD is shown for 18-24 seedlings per genotype for each treatment. Significant differences ($p<0.05$) in hypocotyl lengths with and without AVG are designated by *.

(d) Confirmation of overexpression of *35S:AtCb5-D* in two independent transgenic lines (#5 and #16) compared to the untransformed wild type by semi-quantitative RT-PCR. *Actin7* was used as a loading control. RNA was isolated from rosette leaves of 3-week old plants.

(e) Overexpression of *AtCb5-D* exhibits reduced ethylene sensitivity similar to that conferred by *RTE1* overexpression. Representative 4-day old etiolated seedlings of stable transformants expressing *35S:RTE1* (Resnick et al. 2006) or *35S:AtCb5-D* (line #5) are shown alongside the untransformed wild type. Seedlings were germinated on 1 μM ACC. (f) Hypocotyl lengths of 4-day old etiolated seedlings shows *35S:AtCb5-D* confers reduced ethylene sensitivity. Data is shown for two independent transgenic lines (#5 and #16). Seedlings were germinated on 1 μM ACC. The mean ± SD is shown for 15-27 seedlings per genotype for each treatment. Significant differences ($p<0.05$) between measurements are indicated by different letters above the bars.

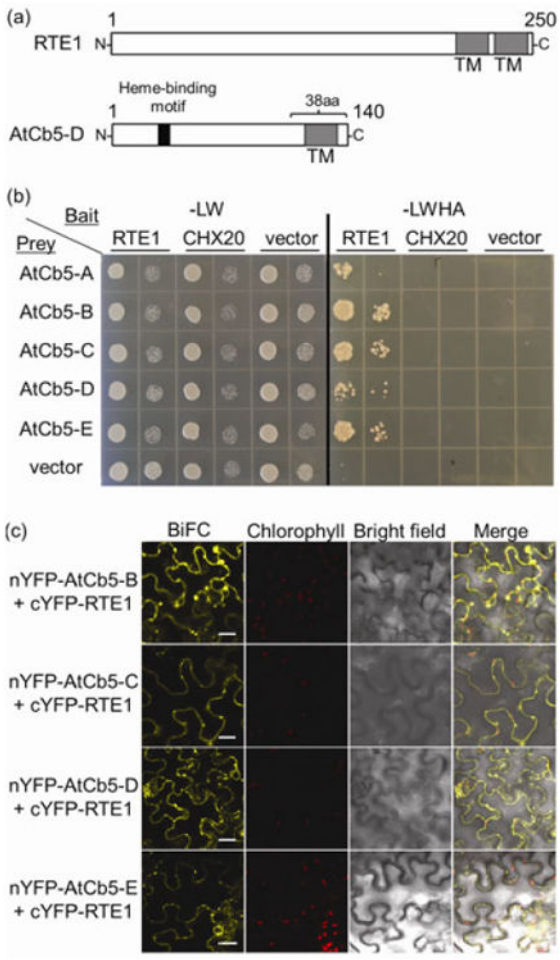

Figure 3. *atcb5* mutant alleles partially suppress *etr1-2* ethylene insensitivity

(a) *atcb5* single mutants suppress *etr1-2* ethylene insensitivity in Arabidopsis seedlings. Comparison of representative 4-day old etiolated seedlings germinated in the absence and presence of 10μM ACC.

(b) Ethylene dose-response analysis of hypocotyl length of 4-day old etiolated seedlings shows partial suppression of *etr1-2* by *atcb5-b, -c and –d*. The mean ± SD is shown for 20-30 seedlings per genotype at each ethylene concentration.

(c) The wild type *AtCb5-D* gene rescues the suppressed phenotype of *etr1-2 atcb5-d.* Representative seedlings are shown for *etr1-2 atcb5-d* transformed with either a genomic DNA fragment (*gAtCb5-D*) containing the entire *AtCb5-D* coding region including ∼1.9kb upstream of the start codon or an *AtCb5-D* cDNA driven by the CaMV 35S promoter (35S:*AtCb5-D*). Representative wild type, *etr1-2* and untransformed *etr1-2 atcb5-d* seedlings are shown for comparison. Seedlings were germinated for 4 days in the dark on 20 μM ACC.

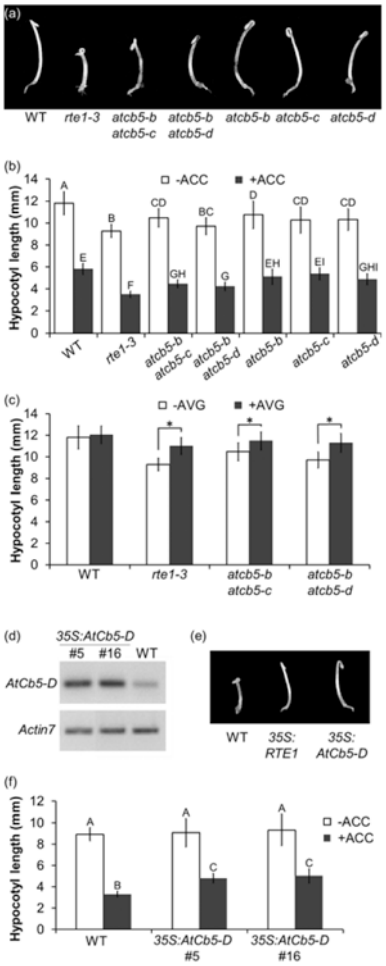

Figure 4. *AtCb5-D* likely acts upstream of *RTE1* in ethylene signaling

(a) Ethylene dose response of hypocotyl lengths in 4-day old etiolated seedlings shows that *rte1* and *rte1-3 atcb5-d* have a similar ethylene response. The mean ± SD is shown for 13-26 seedlings per genotype at each ethylene concentration.

(b) *atcb5-d* does not block the reduced ethylene sensitivity conferred by RTE1 overexpression. Shown are representative 4-day old etiolated seedlings of the wild type and *atcb5-d* mutant before and after transformation with the *35S:RTE1* transgene. Two independent transgenic lines (#1 and #3) are shown for the *atcb5-d* background. Seedlings were germinated on 5μM ACC.

(c) Hypocotyl lengths of 4-day old etiolated seedlings treated with or without 5 μM ACC indicate that *atcb5-d* does not prevent the reduced ethylene sensitivity conferred by *RTE1* overexpression. The mean ± SD is shown for 20-38 seedlings per line for each treatment. Significant differences ($p<0.05$) between measurements are indicated by different letters above the bars.

(d) The *rte1-3* null mutation blocks the reduced ethylene sensitivity conferred by *AtCb5-D* overexpression. Shown are representative 4-day old etiolated seedlings of the wild type and *rte1-3* mutant before and after transformation with the *35S:AtCb5-D* transgene. Two

independent transgenic lines (#10 and #18) are shown for the *rte1-3* background. Seedlings were germinated on 1 μM ACC.

(e) Hypocotyl lengths of 4-day old etiolated seedlings treated with or without 1 μM ACC indicate that *rte1-3* blocks the reduced ethylene sensitivity conferred by *AtCb5-D* overexpression. The mean ± SD is shown for 22-31 seedlings per line for each treatment. Significant differences ($p<0.05$) between measurements are indicated by different letters above the bars.

Table 1

atcb5 mutants partially suppress ethylene insensitivity of *etr1-2* based on chlorophyll content.

	Chlorophyll content (mg/g)		
Genotype	**With ethylene treatment**	**Without ethylene treatment**	**% of no ethylene treatment**
WT	0.025±0.009	0.222±0.009	11.2
etr1-2	0.231±0.018	0.243±0.012	94.8
etr1-2 rte1-3	0.121±0.024	0.277±0.004	43.7
etr1-2 atcb5-b	0.149±0.005	0.249±0.029	60.0
etr1-2 atcb5-c	0.199±0.018	0.326±0.023	61.2
etr1-2 atcb5-d	0.159±0.023	0.278±0.024	57.2

Chlorophyll content was measured as mg per g fresh weight of rosette leaves from 6-week old plants treated for 3 days in a dark, airtight chamber with or without 100 ppm ethylene. Average chlorophyll content was calculated from 3 independent plants. % is the chlorophyll content from plants treated with ethylene as a percentage of chlorophyll content from plants without ethylene treatment.

Table 2

Comparison of the ability of *rte1-2* and *atcb5-d* to suppress ethylene insensitivity conferred by *etr1* dominant mutant transgene alleles.

ETR1 mutation	Suppressed by *rte1-2* [a]	Suppressed by *atcb5-d* (%) [b,]
etr1-2 (A102T) [c]	Yes	Yes (71.4%)
E38A	Yes	Yes (82.8%)
F58A	Yes	Yes (88.8%)
F61A	Yes	Yes (75.6%)
L64A	Yes	Yes (65.9%)
T101A	No	No (99.5%)

[a] Data from Resnick et al. (2008).

[b] Values give hypocotyl length conferred by the *etr1* mutant transgene in the at*cb5-d* background as a percent of that in the wild-type background (data from Figure S5). Seedlings were germinated on 20 μM ACC.

[c] The *etr1-2* allele is a genomic DNA mutant, not a transgene.